Available online at www.sciencedirect.com
SCIENCE DIRECT®
International Journal of Heat and Mass Transfer 48 (2005) 1554–1562
International Journal of HEAT and MASS TRANSFER
www.elsevier.com/locate/ijhmt

Heat transport in Stokes' problem with melting: a two-layer approach

Arup Mukherjee *, John G. Stevens

Department of Mathematical Sciences, Montclair State University, Montclair, NJ 07043, USA

Received 11 September 2004
Available online 15 December 2004

Abstract

We analyze the heat transport from a heated sphere as it melts its way through a solid medium. The work of Emerman and Turcotte [Int. J. Heat Mass Transfer 26 (11) (1983) 1625–1630] is used as a starting point. A thermal layer is added beyond the melt layer to account more accurately for the heat transport to the surrounding medium. This two-layer approach allows us to estimate the extent of the melt region.

PACS: 44.35.+c; 47
Keywords: Stokes' problem; Heat transport; Thermal layer; Integral balance method

1. Introduction

Emerman and Turcotte [4] considered a problem that they aptly termed Stokes' problem with melting. The classical Stokes' problem calculates the drag on a sphere moving at constant velocity through a viscous, fluid medium. "With melting" extends the concept to a sphere embedded in a solid medium. The sphere is provided with a constant heat input that maintains its surface temperature above the melting point of the surrounding medium. The sphere thus "melts its way through" that medium, i.e., the heat transported from the sphere is sufficient to melt a region of the medium around the sphere. The sphere falls through the melted, fluid region, ultimately achieving a steady-state velocity. Emerman and Turcotte were interested in the applications of this problem in geophysics, e.g., magma migration, core formation, and the motion of iron bodies and detached slabs. As they observed, the problem is also related to the so-called China Syndrome, in which a run-away nuclear reactor core melts its way through the earth [15]. The problem is, however, quite general. For example, the medium could be salt, ice, or any solid with a fairly sharp melting point. In the 1960s, well before the publication of [4], several patents were granted for "underground thermal penetrators" using the same principles [1,3]. Indeed, one of them proposed using a nuclear reactor as the heat source. The goal was to drill deep into the earth, in some cases producing a hole by removing the molten rock by means of drilling mud or forced air. An important question that we address in this work is the size of the resulting hole, i.e., the diameter of the cylinder that is melted by the descent of the sphere.

Emerman and Turcotte [4] employed the integral balance method to obtain an approximate solution of the momentum and energy conservation equations in

* Corresponding author.
E-mail addresses: mukherjeea@mail.montclair.edu (A. Mukherjee), stevensj@mail.montclair.edu (J.G. Stevens).

0017-9310/$ - see front matter © 2004 Elsevier Ltd. All rights reserved.
doi:10.1016/j.ijheatmasstransfer.2004.11.003

Nomenclature

We follow the nomenclature used by Emerman and Turcotte [4].

c_p	specific heat capacity of melt
g	acceleration due to gravity
k	thermal conductivity of melt, $\kappa\rho_m c_p$
L	latent heat of fusion
L'	reduced latent heat of fusion, $L + c_p(T_m - T_\infty)$
p	pressure
p_0	pressure at equator
Pe	Peclet number, $u_0 R/\kappa$
Q	total heat flux from the sphere
R	radius of sphere
Ste	Stefan number, $c_p(T_0 - T_\infty)/L'$
t	time
T	temperature
$\mathbf{T}$	dimensionless temperature in molten layer, $(T - T_m)/(T_0 - T_m)$
$\mathscr{T}$	dimensionless temperature in thermal layer, $(T - T_\infty)/(T_m - T_\infty)$
T_m	melting point of medium
T_0	temperature at surface of sphere
T_∞	ambient temperature of medium
u	tangential velocity
$\mathbf{u}$	dimensionless tangential velocity, u/u_0
$\bar{u}$	tangential velocity averaged over the molten layer
u_0	velocity of sphere
v	normal velocity
$\mathbf{v}$	dimensionless normal velocity, v/u_0
x	distance tangential to sphere
y	distance normal to sphere
$\mathbf{y}$	dimensionless distance normal to sphere, y/R
d	molten layer thickness

Greek symbols

δ	dimensionless molten layer thickness, d/R
ε	dimensionless thermal layer thickness
$\Delta\rho$	density difference between sphere and molten medium
η	dynamic viscosity of melt
θ	colatitude
θ^*	colatitude at which lubrication approximation becomes invalid
κ	thermal diffusivity of melt
ρ_m	density of melt
ρ_s	density of sphere

lubrication form. A key result in [4] was an expression for the thickness, d (or δ in dimensionless form), of the molten layer as a function of the colatitude, θ. The relevant geometry is displayed in Fig. 1. That dependence is $\delta(\theta) = \delta_0 \sec(\theta)$, where δ_0 is the thickness at the bottom of sphere (corresponding to $\theta = 0$). The authors observe that as θ increases this expression would give a thickness for which the lubrication approximation would no longer be valid. Indeed, instead of approaching a finite value at the "equator" (corresponding to $\theta = \pi/2$), δ approaches infinity. The colatitude at which the approximation is no longer valid was denoted by θ^*. The contributions to the heat flux and drag from the region $\theta^* \leqslant \theta \leqslant \pi/2$ were shown to be negligible for the range of parameter values of interest. The relationships developed between the power input, terminal velocity, and sphere temperature are thus useful in this regime. The radius of the melted cylinder at the equator will generally be quite close to the radius of the descending sphere. Obviously, the expression obtained in [4] for $\delta(\theta)$ cannot provide an estimate for difference between these radii.

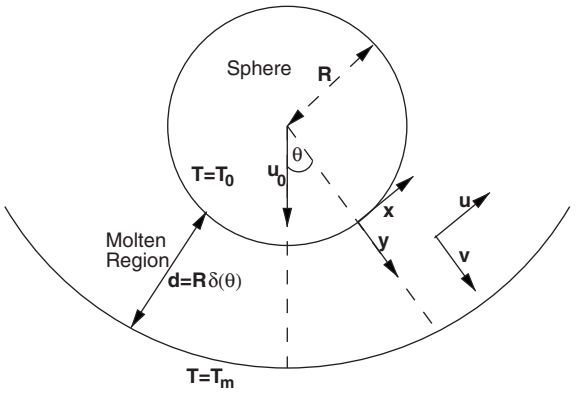

Fig. 1. Geometry for Stokes' problem with melting.

In the intervening years several investigators have worked on closely related problems. The problem of Stokes's flow with strongly temperature-dependent viscosity in a fluid is also closely related to ours and was studied experimentally and analytically by Morris and coauthors [14,2]. In [14], the drag on and the heat flux out of a hot sphere moving steadily in a fluid with strongly temperature-dependent viscosity is determined analytically, while [2] studies a closely related problem experimentally and analytically. The current paper deals with a hot sphere moving through a fluid whose viscosity is assumed to be constant. In some cases, incorporating the effects of temperature-dependent viscosity in the context of the problem we study could be of considerable interest. Moallemi and Viskanta have studied the melting around a moving heat source experimentally

[10,11] and theoretically [12,13]. They developed detailed mathematical models and solved them using numerical integration. Heat transport and flow in the molten wake of the sphere were included. Reasonably good agreement between simulation and experimental results was obtained, although some systematic departure in heat source velocity was noted. Calculation of the solid–liquid interface using this numerical approach gives a finite, realistic value for the melt layer thickness at the equator of a moving sphere.

In this paper, we investigate the question of whether an estimate for this thickness can be obtained by essentially analytical means similar to those employed by Emerman and Turcotte. We show that the singularity in $\delta(\theta)$ at $\pi/2$ is not due to the lubrication approximation. It is really an effect of the way in which heat transport to the surrounding medium was treated. We surround the melt layer with a thermal layer that makes possible a more accurate description of heat transport to the surrounding solid medium. We demonstrate that this novel two-layer approach results in a finite value for $\delta(\pi/2)$. In addition, the power required to achieve a given terminal velocity is somewhat greater than that obtained from the Emerman and Turcotte model for moderately large values of the Peclet number. Our computations suggest that this difference becomes smaller as the Peclet number increases. The basic approach employed by Emerman and Turcotte is outlined in Section 2.1. In Section 2.2 we describe the details of our new two-layer approach. The algebraic manipulations associated with the integral balance method, which in our case is employed twice, are accomplished using the computer algebra system Maple. These Maple work sheets are available from the authors upon request. The dependence of δ on the colatitude θ is obtained by the numerical solution of an ordinary differential equation. In Section 3 we provide a detailed example of how our analysis and results compare with those of Emerman and Turcotte.

2. Model and analysis

The geometry of the problem is displayed in Fig. 1. Under the assumptions outlined in this section, the molten layer thickness $d(\theta)$ (or $\delta(\theta)$ in dimensionless form) is given by Eq. (8) where θ represents the colatitude and *Ste* and *Pe* are the Stefan and Peclet numbers. In Section 2.1, we follow Emerman and Turcotte [4] in deriving this expression based on the conservation of momentum, mass, and energy in approximate forms valid when $\delta(\theta) \ll 1$. The computations leading to the final expression for the melt layer thickness provide insight into the reason for its observed anomalous behavior near the equator and lead directly to our two-layer approach of Section 2.2. Our two-layer approach introduces a thermal layer as shown in Fig. 2. The dimensionless

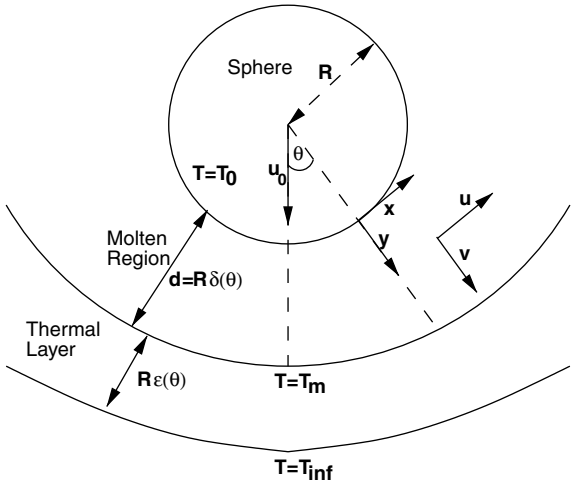

Fig. 2. Geometry for Stokes' problem with melting with thermal layer added.

thermal layer thickness $\varepsilon(\theta)$ satisfies Eq. (16). Because we need an analytic expression for $\varepsilon(\theta)$, we use an accurate series solution for Eq. (16). The assumptions and details of our approach are given in Section 2.2.

2.1. The Emerman and Turcotte model

Under the lubrication assumption, the Navier–Stokes equation becomes (see, for example, [16]) $\eta \frac{\partial^2 u}{\partial y^2} = \frac{\mathrm{d}p}{\mathrm{d}x}$, with boundary conditions $u(0) = 0$ and $u(d) = 0$, where $u = u(y)$ is the tangential component of velocity in the molten layer. We assume that the pressure in the molten layer, $p = p(x)$, depends only on x and that the thickness of the molten layer, $d = d(\theta)$, is a function of the colatitude $\theta = x/R$. Because the molten layer/solid medium interface is in essence a moving wall, $u(d) = u_0 \sin\theta$ seems to be the correct boundary condition. In what follows we work under the assumption that $d \ll R$, so that $u \gg u_0$ throughout most of the melt region. The boundary condition $u(d) = 0$ is consistent with these assumptions as pointed out in [4]. We have investigated the use of the modified boundary condition $u(d) = u_0 \sin\theta$ and find that it results in much greater complexity while not significantly affecting the results. Details of our investigation of this issue are presented in Appendix A. The boundary value problem for u is solved to obtain $u = \frac{1}{2\eta}(\frac{\mathrm{d}p}{\mathrm{d}x}) y(y-d)$. Equating the mass flux ahead of the sphere to the mass flux about the sphere using conservation of mass, we obtain $\pi(R\sin\theta)^2 u_0 = 2\pi R d\bar{u}\sin\theta$, where $\bar{u}$ represents the average velocity over the molten layer. Solving for $\bar{u}$ and using the definition we arrive at $\frac{u_0 R}{2d}\sin\theta = \bar{u} = \frac{1}{d}\int_0^d u\,\mathrm{d}y = \frac{-d^2}{12\eta}\frac{\mathrm{d}p}{\mathrm{d}x}$. Substituting the pressure gradient from the last equation in the velocity expression above, we obtain $u = -\frac{3Ru_0}{d^3} y(y-d)\sin\theta$.

The equation of continuity in boundary layer form for flow over a sphere is (see, for example, [16]) $\frac{\partial}{\partial x}(u\sin\theta)+\sin\theta\frac{\partial v}{\partial y}=0$, where $v=v(y)$ represents the normal component of the velocity in the molten layer. At this point, Emerman and Turcotte employed the continuity equation to obtain an expression for $v(d)$, the normal component of the velocity at the interface. Finally, the equation for conservation of energy in boundary layer form is used to determine $d=d(\theta)$. Following [16], when $d\ll R$, the steady-state energy equation is $u\frac{\partial T}{\partial x}+v\frac{\partial T}{\partial y}=\kappa\frac{\partial^2 T}{\partial y^2}$.

As an alternative to direct solution, we will integrate the energy equation over the molten layer to obtain an ordinary differential equation in δ. This approach is closely related to the integral method of boundary layer theory (see for example, [16]) and the integral balance method for heat conduction (see for example, [8]). We employ dimensionless variables defined via the following transformations: $\theta=x/R$, $\mathbf{y}=y/R$, $\delta=d/R$, $\mathbf{u}=u/u_0$, $\mathbf{v}=v/u_0$, and $\mathbf{T}=(T-T_{\mathrm{m}})/(T_0-T_{\mathrm{m}})$. Boldface symbols represent dimensionless quantities with the following exception: the colatitude θ is unchanged and the thickness of the molten layer is represented by $\delta(\theta)$ in dimensionless form. By direct substitution, we arrive at $\mathbf{u}=-(3/\delta^3)\sin\theta\mathbf{y}(\mathbf{y}-\delta)$, the dimensionless continuity equation $\frac{\partial}{\partial\theta}(\mathbf{u}\sin\theta)+\sin\theta\frac{\partial\mathbf{v}}{\partial\mathbf{y}}=0$, and the dimensionless energy equation $\mathbf{u}\frac{\partial\mathbf{T}}{\partial\theta}+\mathbf{v}\frac{\partial\mathbf{T}}{\partial\mathbf{y}}=\frac{1}{Pe}\frac{\partial^2\mathbf{T}}{\partial\mathbf{y}^2}$, where $Pe=u_0R/\kappa$ is the Peclet Number. Multiplying the dimensionless energy equation by $\sin\theta$, integrating with respect to $\mathbf{y}$ from 0 to δ, using integration by parts on the second integral on the left hand side, and noting that $\mathbf{v}\mathbf{T}\sin\theta|_0^\delta=0$ (because $\mathbf{v}(0)=\mathbf{T}(\delta)=0$) yields

$$\int_0^\delta \mathbf{u}\sin\theta\frac{\partial\mathbf{T}}{\partial\theta}\mathrm{d}\mathbf{y}-\int_0^\delta\mathbf{T}\left(\sin\theta\frac{\partial\mathbf{v}}{\partial\mathbf{y}}\right)\mathrm{d}\mathbf{y}=\frac{\sin\theta}{Pe}\left(\left.\frac{\partial\mathbf{T}}{\partial\mathbf{y}}\right|_\delta-\left.\frac{\partial\mathbf{T}}{\partial\mathbf{y}}\right|_0\right). \tag{1}$$

We observe that because $\mathbf{T}(\delta)=0$, the aforementioned expression for $v(d)$ (or $\mathbf{v}(\delta)$ in dimensionless form) is not required. Using the dimensionless continuity equation together with standard integral equalities and the condition $\mathbf{T}(\delta)=0$ for the second term on the left hand side leads to the final integral formulation

$$\frac{\partial}{\partial\theta}\int_0^\delta\mathbf{u}\sin\theta\mathbf{T}\mathrm{d}\mathbf{y}=\frac{\sin\theta}{Pe}\left(\left.\frac{\partial\mathbf{T}}{\partial\mathbf{y}}\right|_\delta-\left.\frac{\partial\mathbf{T}}{\partial\mathbf{y}}\right|_0\right). \tag{2}$$

Emerman and Turcotte then used a quadratic polynomial in $\mathbf{y}$ for the temperature profile in the molten layer based on the boundary conditions

$$T(0)=T_0\Longleftrightarrow\mathbf{T}(0)=1, \tag{3}$$

$$T(d)=T_{\mathrm{m}}\Longleftrightarrow\mathbf{T}(\delta)=0, \tag{4}$$

$$\left.\frac{\partial T}{\partial y}\right|_{y=d}=-\frac{\rho_{\mathrm{m}}u_0L'}{k}\cos\theta\Longleftrightarrow\left.\frac{\partial\mathbf{T}}{\partial\mathbf{y}}\right|_{\mathbf{y}=\delta}=-\frac{Pe}{Ste}\cos\theta \tag{5}$$

where $T=T(y)$ and $\mathbf{T}=\mathbf{T}(\mathbf{y})$ represent the temperature profiles, and $Ste=c_p(T_0-T_\infty)/L'$ is the Stefan number. The use of higher order polynomials for the temperature was investigated by Fengya and Stevens [5]. They used a cubic temperature profile and investigated the dependence of the molten layer thickness on this choice and the Stefan number. However, for the range of values of the Stefan number most frequently encountered (small Ste), the differences were shown to be minor.

As we shall see, the boundary condition (5) leads to certain anomalies. This condition accounts for the heat required to raise the temperature of the solid medium within the control volume from T_∞ to T_{m} and to melt the solid medium, but fails to incorporate the heat transfer by conduction through the sides. The loss of accuracy occurs as θ approaches $\pi/2$. If d were to approach a finite value, then the heat loss to the medium outside a cylinder of radius $R+d(\pi/2)$ would be neglected. We shall see that the use of this boundary condition leads to $d\to\infty$ as $\theta\to\pi/2$.

The analysis of Emerman and Turcotte yields many useful results which we now outline. In the next section, we will compare and contrast these with those based on a different boundary condition which we derive from our two-layer approach.

The quadratic function for $\mathbf{T}$ satisfying the boundary conditions (3)–(5) is

$$\mathbf{T}=1+\mathbf{y}\left(\frac{Pe}{Ste}\cos\theta-\frac{2}{\delta}\right)+\mathbf{y}^2\left(\frac{1}{\delta^2}-\frac{Pe}{Ste}\frac{\cos\theta}{\delta}\right). \tag{6}$$

Because $\frac{\partial^2\mathbf{T}}{\partial\mathbf{y}^2}|_{\mathbf{y}=0}=0$, by substituting $\mathbf{y}=0$ in the dimensionless energy equation, the coefficient of $\mathbf{y}^2$ in Eq. (6) must vanish. This observation immediately leads to the expression $\delta=\delta(\theta)=Ste/(Pe\cos\theta)$, which we will compare with the expression obtained using the integral method below.

Substituting the quadratic temperature profile from (6) into the integral formulation (2) we obtain the following differential equation for the molten layer width $\delta(\theta)$

$$\frac{\mathrm{d}\delta}{\mathrm{d}\theta}=\frac{20Ste-Pe^2\delta^2-20Pe\delta\cos\theta-3Pe^2\delta^2\cos^2\theta-3StePe\delta\cos\theta}{Pe^2\delta\sin\theta\cos\theta}. \tag{7}$$

Because $\frac{\mathrm{d}\delta}{\mathrm{d}\theta}|_{\theta=0}=0$ by symmetry and because $\sin\theta$ appears in the denominator of the differential equation, $\delta(0)$ must be chosen to make the numerator of (7) vanish as $\theta\to0$. Choosing the positive root of the quadratic in δ obtained by setting $\theta=0$ in the numerator leads to the initial condition $\delta(0)=\frac{f(Ste)}{Pe}$ where $f(z)=0.25(-3z-20+\sqrt{9z^2+280z+400})$. Solving Eq. (7) subject to this initial condition yields

$$\delta(\theta) = \frac{d(\theta)}{R} = \delta(0)\sec\theta = \frac{f(Ste)}{Pe}\sec\theta. \tag{8}$$

It is easily verified that as $Ste \to 0$, $f(Ste)/Ste \to 1$. Thus, the expression for the molten layer thickness deduced directly from the dimensionless energy equation is consistent with the result from the integral method for small values of *Ste*. The expression for the width of the molten layer obtained in (8) following the boundary conditions used by Emerman and Turcotte shows that the width of the molten layer, δ, goes to ∞ as the colatitude, θ, approaches $\pi/2$. Obviously, this model is unsuitable for estimating the size of the cylinder of medium that melts.

The dimensionless power consumption, $\mathbf{Q}$, obtained by neglecting the heat flux through the hemisphere away from the direction of travel, is

$$\mathbf{Q} = \frac{Q}{\pi R^2 \rho u_0 L'} = -\frac{2\ Ste}{Pe}\int_0^{\pi/2} \left.\frac{\partial \mathbf{T}}{\partial \mathbf{y}}\right|_{\mathbf{y}=0} \sin\theta \mathrm{d}\theta = \frac{2Ste}{f(Ste)} - 1, \tag{9}$$

where Q is the total heat flux from the sphere. As $Ste \to 0$, $\mathbf{Q}$ approaches 1, i.e., $Q \to \pi R^2 \rho u_0 L'$, the power required to melt a cylinder of radius R advancing at a velocity u_0. This expression clearly excludes any heat loss to the surrounding rock and underpredicts the power required for some cases, especially when $T_\mathrm{m} - T_\infty$ is large.

2.2. Including heat loss to the environment: A two-layer approach

The anomaly observed above stems from the boundary condition (5). Notice that as θ approaches $\pi/2$, the gradient $\frac{\partial T}{\partial y}|_{y=d}$ approaches zero. This behavior is not consistent with the temperature at this point being T_m and that of the surrounding medium being T_∞. An improved boundary condition at this solid–liquid interface, based on the requirement that the latent heat required to melt the solid must be supplied by conduction is

$$\left[k\frac{\partial T}{\partial y}\right] = k_\mathrm{s}\frac{\partial T_\mathrm{s}}{\partial y} - k_\mathrm{l}\frac{\partial T_\mathrm{l}}{\partial y} = L\rho u_0 \cos\theta, \quad \text{at } y = d \tag{10}$$

where $[\cdots]$ denotes the jump and the subscripts s and l represent quantities associated with the solid and molten (liquid) medium, respectively. To apply the boundary condition (10) we need to compute $\frac{\partial T_\mathrm{s}}{\partial y}$. To this end, we consider a thermal layer beyond the melt region as shown in Fig. 2. The temperature in the thermal layer varies from the melting point of the medium, T_m, at the melt/solid interface to the ambient temperature of the solid medium, T_∞, at its outer boundary. The coordinate system of the molten layer is extended into the thermal layer and the variable y is re-mapped so that it is zero at the interface between the molten and thermal layers. The notations are the same as before and we let $\varepsilon = \varepsilon(\theta)$ represent the dimensionless thickness of this thermal layer. We introduce the non-dimensional temperature $\mathscr{T} = (T_\mathrm{s} - T_\infty)/(T_\mathrm{m} - T_\infty)$ for the thermal layer. Using the relation $k_l = \rho_m c_p \kappa$, the boundary condition (10) in dimensionless form is

$$\frac{\partial \mathbf{T}}{\partial \mathbf{y}} = -\frac{Pe}{\sigma}\cos\theta + \beta\frac{\partial \mathscr{T}}{\partial \mathbf{y}}, \tag{11}$$

where

$$\beta = \frac{k_\mathrm{s}(T_\mathrm{m} - T_\infty)}{k_\mathrm{l}(T_0 - T_\mathrm{m})}, \quad \text{and} \quad \sigma = \frac{c_p(T_0 - T_\mathrm{m})}{L}. \tag{12}$$

The quantity σ is analogous to *Ste* but is based on the actual latent heat. In our calculations, we shall assume $k_\mathrm{s} = k_l$. We will now use the integral balance approach on the thermal layer to find a differential equation for ε, solve the equation using suitable initial conditions, and use the solution to compute $\frac{\partial \mathscr{T}}{\partial \mathbf{y}}$.

Using $u = u_0 \sin\theta$ and $v = -u_0\cos\theta$ for the velocity in the energy equation applied to the thermal layer, and changing to dimensionless form using $\mathscr{T}$ yields

$$\sin\theta\frac{\partial \mathscr{T}}{\partial \theta} - \cos\theta\frac{\partial \mathscr{T}}{\partial \mathbf{y}} = \frac{1}{Pe}\frac{\partial^2 \mathscr{T}}{\partial \mathbf{y}^2}. \tag{13}$$

Integrating the above equation, using the integral identity

$$\frac{\partial}{\partial\theta}\int_0^\varepsilon \mathscr{T}\mathrm{d}\mathbf{y} = \frac{\mathrm{d}\varepsilon}{\mathrm{d}\theta}\mathscr{T}(\varepsilon) + \int_0^\varepsilon \frac{\partial \mathscr{T}}{\partial\theta}\mathrm{d}\mathbf{y}, \tag{14}$$

and the boundary conditions, $\mathscr{T}(0) = 1$, $\mathscr{T}(\varepsilon) = 0$, and $\frac{\partial \mathscr{T}}{\partial \mathbf{y}}|_{\mathbf{y}=\varepsilon} = 0$, yields the integral balance

$$\sin\theta\frac{\partial}{\partial\theta}\int_0^\varepsilon \mathscr{T}\mathrm{d}\mathbf{y} + \cos\theta = -\frac{1}{Pe}\left.\frac{\partial \mathscr{T}}{\partial \mathbf{y}}\right|_{\mathbf{y}=0}. \tag{15}$$

Assuming a quadratic temperature profile in the thermal layer, we obtain $\mathscr{T}(\mathbf{y}) = 1 - 2(\mathbf{y}/\varepsilon) + (\mathbf{y}^2/\varepsilon^2)$. Substituting in the integral balance equation (15), we find that the thermal layer thickness, ε, satisfies the differential equation

$$\frac{\mathrm{d}\varepsilon}{\mathrm{d}\theta} = \frac{6 - 3\varepsilon Pe\cos\theta}{\varepsilon Pe\sin\theta}. \tag{16}$$

Since $\frac{\mathrm{d}\varepsilon}{\mathrm{d}\theta}|_{\theta=0} = 0$ and $\sin\theta$ appears in the denominator, the initial condition on ε must be $\varepsilon(0) = 2/Pe$.

Eq. (16) is an Abel's equation of the second kind which can be transformed into an Abel's equation of the first kind using standard transformations (see, for example, [7]). The most general known solution method for Abel's equations of the first kind due to M. Chini are outlined in [7]. We were unable to obtain explicit closed form solutions to Eq. (16) following these methods because we were not able to evaluate resulting integrals in closed form, even using Maple. As an alternative, we use a series approximation for $\varepsilon(\theta)$ which yields the required expression for $\frac{\partial \mathscr{T}}{\partial \mathbf{y}}|_{\mathbf{y}=0}$. We have carefully explored series solutions using various orders and com-

pared our series solutions with a numerical (exact) solution.

When θ is not near $\pi/2$, the relative errors between the series and exact (numerical) solutions are small independent of the order. The maximum relative error occurs at $\theta = \pi/2$ independent of the order of approximation and the value of Pe. For example, if $Pe = 10.0$, the order-4 series solution produces a relative error of 0.0413 when $\theta = \pi/4$, while the order-6 and order-8 approximations yield relative errors of 0.0044 and 0.0001 respectively. For the same Peclet number, the relative errors corresponding to $\theta = \pi/2$ are 0.3523, 0.1097, and 0.0039 respectively. When the radius, R, of the sphere is 3 cm and the total heat flux out of the sphere, Q, is 5000 W, the Peclet number is $Pe = 10.33$. These are the values used in our worked example in Section 3. The series approximations of different orders all under predict the thickness of the thermal layer, $\varepsilon(\theta)$, resulting in a conservative estimate for the temperature gradient. A detailed listing of relative errors for the order-4, order-6, and order-8, series approximations at different θ values using a the values 5.0, 10.0, and 15.0 for Pe are given in Appendix B. Although we use the order-4 series approximation for our discussion in the rest of this section for the sake of simplicity of the expressions involved, it is a simple step to extend our analysis using higher order series approximations for Eq. (16). In fact, we use the order-8 approximation for our worked example in Section 3.

Substituting the order-4 series approximation

$$\varepsilon(\theta) = \frac{2}{Pe} + \frac{3}{3\ Pe + 4}\theta^2 + \mathrm{O}(\theta^4), \tag{17}$$

in the quadratic temperature profile leads to

$$\frac{\partial \mathscr{T}}{\partial \mathbf{y}} = -\frac{6Pe^2 + 8Pe}{8 + 6Pe + 3Pe\theta^2}. \tag{18}$$

Using this expression in the dimensionless boundary condition (11) results in

$$\frac{\partial \mathbf{T}}{\partial \mathbf{y}} = -\frac{Pe}{\sigma}\cos\theta - \frac{\beta(6Pe^2 + 8Pe)}{8 + 6Pe + 3Pe\theta^2}. \tag{19}$$

Notice that the first term on the right hand side of the last expression closely resembles the boundary condition (5) used by Emerman and Turcotte. The only difference is that $\sigma = (c_p/L)(T_0 - T_\mathrm{m})$, which appears in (19), does not include the heat required to bring the solid medium up to a temperature of T_m; this is included in $Ste = (c_p/L')(T_0 - T_\mathrm{m})$ which Emerman and Turcotte use in (5). Also, using the condition (19) guarantees that $\frac{\partial \mathbf{T}}{\partial \mathbf{y}} \neq 0$ as $\theta \to \pi/2$.

The integral method based on the integral balance (2) and a quadratic temperature profile based on the conditions (3)–(5) is now repeated using our two-layer approach. The only change is the replacement of condition (5) by the improved (two-layer) condition (19). We have been unable to obtain closed-form solutions for the molten layer thickness $\delta(\theta)$ using the two-layer approach. In fact, the differential equation satisfied by δ is quite complicated. Thus, for given values of Pe, σ, and β, we compute $\delta(\theta)$ numerically. The molten layer thickness, δ, obtained using the two approaches agree very closely for small values of θ. However, $\delta(\pi/2)$ obtained using the two-layer approach is finite.

3. A worked example

In this section we present sample calculations that illustrate the differences in the results based on the boundary condition in Eq. (5) and those obtained using the two-layer approach. First, we discuss the relevant variables and their relationships. As is evident from the nomenclature, there are many variables for which values must be specified. Most of these values are determined as physical properties of the solid medium and the material composing the heated sphere. Following Emerman and Turcotte [4], we have used properties for the solid medium that are typical for "rock," for example, basalt. We have taken the sphere to have a radius of 3 cm, representative of a small rock penetrator. The values for the relevant physical properties are given in Table 1.

Several important variables do not relate directly to physical properties that can be easily determined. They are Q, the rate of heat supplied to (and in the steady-state the total flux leaving) the sphere; u_0, steady-state velocity of the sphere; and T_0, the surface temperature of the sphere. The values for these variables must be determined from two balances once the value for one of them has been specified. For the rock penetrator we consider here, Q, the rate of heat input to the sphere, is most easily set. It is, however, possible to specify either u_0 or T_0 and then determine Q and the remaining variable. The heat flux from the sphere is given in Eq. (9).

The equality of the drag and buoyancy forces acting on the sphere provides the second steady state relationship or the force balance. As observed in [4], if

Table 1
Properties used in sample calculations

Variable	Value
R	3 cm
η	10 Pa s
T_∞	298 K
c_p	1.046 kJ/(kg · K)
L	418 kJ/kg
T_m	1473 K
κ	1×10^{-6} m^2/s
ρ_m	2700 kg/m^3
ρ_s	9000 kg/m^3

$\delta = d/R \ll 1$, then the drag force due to shear stress is negligible compared to that due to pressure, giving

$$F_d = 2\pi R^2 \int_0^{\pi/2} (p - p_0)\cos\theta \sin\theta \, d\theta, \tag{20}$$

where p_0 is the pressure at $\theta = \pi/2$, assumed to be uniform over $\pi/2 \leqslant \theta \leqslant \pi$. The buoyancy force is

$$F_b = \frac{4}{3}\pi R^3 g \Delta\rho, \tag{21}$$

and $F_d = F_b$ gives the requisite force balance. The θ-dependence of $\frac{\partial T}{\partial y}|_{y=0}$ can be determined from the temperature profile (6) upon differentiating with respect to **y** once $\delta(\theta)$ is known. Likewise, the θ-dependence of $p - p_0$ can be obtained by integrating $\frac{u_0 R}{2d}\sin\theta = \frac{1}{d}\int_0^d u\,dy = \frac{-d^2}{12\eta}\frac{dp}{dx}$ given $d(\theta) = R\delta(\theta)$. For the purpose of this comparison, we denote the expression for $\delta(\theta)$ from the Emerman and Turcotte model given in Eq. (8) by $\delta_{\mathbf{ET}}$. The dependence of δ on θ resulting from the 2-layer approach will be designated $\delta_{\mathbf{2L}}$. As shown in Section 2.1, $\delta_{\mathbf{ET}}(\theta)$ depends only on the dimensionless groups *Pe* and *Ste*. In Section 2.2 it is demonstrated that $\delta_{\mathbf{2L}}(\theta)$ depends only on *Pe*, σ, and β. All of these dimensionless parameters depend only on u_0 and T_0, in addition to the known material properties given in Table 1. Thus if the rate of heat input to the sphere, Q, is known, the heat and force balances form a system of two nonlinear equations for u_0 and T_0. In all cases that we have examined only one solution of this system yields physically meaningful values. The closed form for $\delta_{\mathbf{ET}}(\theta)$ lends itself well to this determination. In the two-layer approach, the same two balances can be solved to obtain u_0 and T_0, but doing so is somewhat more complicated because $\delta_{\mathbf{2L}}(\theta)$ is obtained by solving an ordinary differential equation numerically.

Here we give a comparison based on values for u_0 and T_0 computed from the balances derived using Eq. (8). Using the values listed in Table 1 and a total heat flux $Q = 5000$ W, the velocity was found to 3.445×10^{-4} m/s (2.067 cm/min) with a sphere temperature of 1973 K. The resulting values of 10.33 and 0.3177 for *Pe* and *Ste* completely determine $\delta_{\mathbf{ET}}(\theta)$. It is instructive to use the same values for u_0 and T_0 to obtain $\delta_{\mathbf{2L}}(\theta)$ for the two-layer model. The corresponding values for σ and β are 1.252 and 2.349, respectively. In Fig. 3, the graphs of both $\delta_{\mathbf{ET}}(\theta)$ and $\delta_{\mathbf{2L}}(\theta)$ are shown. The innermost curve in the figure represents the boundary of the sphere and the middle line shows $\delta_{\mathbf{2L}}$. The eighth order approximation for $\varepsilon(\theta)$ was used for these calculations. The values for $\delta_{\mathbf{ET}}(0)$ and $\delta_{\mathbf{2L}}(0)$ found by requiring the numerator of the respective expression for $\frac{d\delta}{d\theta}$ to vanish at $\theta = 0$ are identical to nine significant digits. The value is approximately 0.0285, validating the assumption $\delta \ll 1$ and giving a melt layer thickness there of approximately 0.86 mm. Further, we observe the near perfect agreement between $\delta_{\mathbf{ET}}(\theta)$ and $\delta_{\mathbf{2L}}(\theta)$ for θ from 0 to approximately $\pi/3$. This congruity is striking because of the different ways in which they are obtained, i.e, the equations that determine them are quite dissimilar in form. Moreover, because $\delta_{\mathbf{ET}}$ and $\delta_{\mathbf{2L}}$ are nearly equal over $0 \leqslant \theta \leqslant \theta^*$, it is reasonable to expect that the integrals in Eqs. (9) and (20) would not differ appreciably if $\delta_{\mathbf{2L}}$ were used instead of $\delta_{\mathbf{ET}}$. We further examine the heat balance below. The salient difference between $\delta_{\mathbf{ET}}$ and $\delta_{\mathbf{2L}}$ is evident as θ approaches $\pi/2$. As we know, $\delta_{\mathbf{ET}}$ becomes infinite, indicating a physically unrealistic unbounded melt region. In contrast, $\delta_{\mathbf{2L}}(\pi/2) = 0.1325$, a finite value that is still consistent with the use of the lubrication approximation. The predicted cross-sectional area of the melt region is approximately 28% larger than the projected area of the sphere. Thus the use of the boundary condition in Eq. (19) obtained by adding the thermal layer to account for heat transport to the surroundings eliminates the anomalous singularity evident in $\delta_{\mathbf{ET}}$.

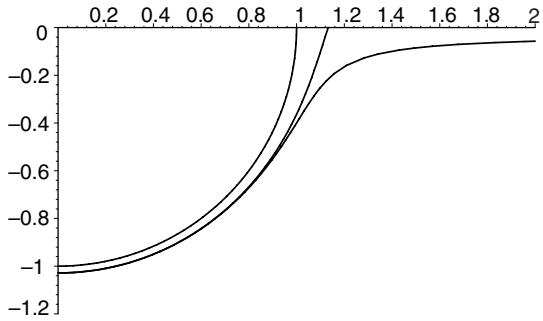

Fig. 3. Comparison of $\delta_{\mathbf{ET}}(\theta)$ and $\delta_{\mathbf{2L}}(\theta)$.

Finally, we examine the total heat flux from the sphere given by the integration indicated in Eq. (9) using $\delta_{\mathbf{2L}}$ to determine $\frac{\partial T}{\partial y}|_{y=0}$ instead of $\delta_{\mathbf{ET}}$. The tedious computations involved were carried out with comparative ease using the numerical and symbolic capabilities of Maple. For the case discussed above, 5765 W was obtained for Q. This value is moderately higher than the value of 5000 W used to obtain the values for u_0 and T_0 employing Eq. (9) based on $\delta_{\mathbf{ET}}$. We observe that the gradient $\frac{\partial T}{\partial y}|_{y=0}$ derived from $\delta_{\mathbf{ET}}(\theta)$ vanishes as θ approaches $\pi/2$, but approaches a non-zero value in the two-layer approach. The increase in the indicated total heat flux is thus due to the additional radial heat loss to the surrounding medium. In our computational investigations, we have observed that the difference in the power from the two approaches diminishes as *Pe* becomes larger.

4. Summary and conclusions

In [4], Emerman and Turcotte obtained an elegant solution for the thickness of the molten layer

surrounding a heated sphere as it steadily melts its way through a solid medium. The closed-form expression that they derived for this function of colatitude, $\delta_{\mathbf{ET}}(\theta)$ as given in (8), facilitated the evaluation of the integrals required to compute the heat flux from the sphere and the drag that it experiences. However, the solution exhibits a non-physical singularity, i.e., the thickness tends to infinity as the equator is approached. In this paper we have shown that the origin of this singularity is the use of a boundary condition that does not include heat loss to the surrounding medium beyond the portion that is eventually melted.

In order to account for such heat transport, the integral balance method of Goodman [6] was employed across a thermal layer that extends beyond the melt region. The determination of the thickness of that thermal layer, found as a truncated series solution, provided an expression for the temperature gradient in the solid at the melt interface. The exact boundary condition (10) could then be employed. The integral balance method was then applied to the melt layer using the temperature profile determined from this boundary condition. The resulting differential equation for the melt thickness was solved numerically to obtain the solution, $\delta_{\mathbf{2L}}(\theta)$, based on our two-layer approach.

The comparison between $\delta_{\mathbf{ET}}(\theta)$ and $\delta_{\mathbf{2L}}(\theta)$ for the case shown in Fig. 3 is instructive. The agreement between the two until quite close to the equator is noteworthy. For this example, the heat flux from the sphere based on $\delta_{\mathbf{2L}}$ was calculated to be 5765 W, compared to 5000 W obtained using $\delta_{\mathbf{ET}}$. The increase is due to additional radial heat loss to the surroundings. In the context of the overall agreement, it is noteworthy that the singularity in the melt thickness has been resolved using the two-layer approach.

Appendix A. Boundary condition at molten layer/rock interface

As mentioned in Section 2.1, the boundary condition $u(d) = u_0 \sin\theta$ is more appropriate than $u(d) = 0$ at the molten layer/solid medium interface. However, when $d \ll R$, using either boundary condition yields no discernable difference in the results. Note that, for the purposes of this section, we do not use the thermal layer introduced in Section 2.2. For example, if we were to use the parameters from Section 3 and compute the dimensionless width of the molten layers using the two different boundary conditions for $u(d)$, the answers are almost identical even when θ is very close to $\pi/2$. In particular, we obtain 0.947×10^{-3} for $\delta(\pi/3)$ using the boundary condition $u(d) = 0$ and 0.948×10^{-3} using $u(d) = u_0 \sin\theta$. Even for $\delta(\pi/2.2)$ we obtain 0.333×10^{-2} and 0.337×10^{-2}, respectively. We have used the dimensionless analog of the simpler boundary condition, $u(d) = 0$, for our two-layer approach in Section 2.2.

Appendix B. Series solution for the thermal layer

We use $\varepsilon_j(\theta)$ to represent the order-j series solution of Eq. (16) subject to the initial condition $\varepsilon(0) = 2/Pe$, and $\varepsilon_{\mathrm{ex}}(\theta)$ to represent the exact (numerical) solution. The relative error associated with $\varepsilon_j(\theta)$ will be represented as $E_j(\theta)$ and defined in the usual way as

$$E_j(\theta) = \left| \frac{\varepsilon_j(\theta) - \varepsilon_{\mathrm{ex}}(\theta)}{\varepsilon_{\mathrm{ex}}(\theta)} \right|. \tag{B.1}$$

The expressions for $\varepsilon_4(\theta)$, $\varepsilon_6(\theta)$, and $\varepsilon_8(\theta)$ are

$$\varepsilon_4(\theta) = \frac{2}{Pe} + \frac{3}{3\ Pe + 4}\theta^2 + \mathrm{O}(\theta^4), \tag{B.2}$$

$$\varepsilon_6(\theta) = \frac{2}{Pe} + \frac{3}{3Pe + 4}\theta^2 + \frac{45Pe^2 + 16}{4(27Pe^3 + 144Pe^2 + 240Pe + 128)}\theta^4 + \mathrm{O}(\theta^6), \tag{B.3}$$

and

$$\varepsilon_8(\theta) = \frac{2}{Pe} + \frac{3}{3Pe+4}\theta^2 + \frac{45Pe^2+16}{4(27Pe^3+144Pe^2+240Pe+128)}\theta^4 + \frac{128Pe + 3696Pe^2 - 4608Pe^3 + 1647Pe^4 + 512}{120(5888Pe + 6528Pe^2 + 864Pe^4 + 3456Pe^3 + 81Pe^5 + 2048)}\theta^6 + \mathrm{O}(\theta^8). \tag{B.4}$$

The relative errors $E_j(\theta)$ for $j = 4, 6$, and 8 are listed in Table B.1 for $\theta = \pi/4$, $\theta = \pi/3$, and $\theta = \pi/2$. We have used three representative values of Pe for our calculations.

As expected, $\max_{0 \leqslant \theta \leqslant \pi/2} E_j(\theta)$ occurs at $\theta = \pi/2$ independent of Pe and the order of approximation j. We also observe that Pe has a nearly linear relationship with the radius, R, and power, Q. Thus, depending on the parameters of a physical problem, the analysis of Section 2.2

Table B.1
Relative errors $E_j(\theta)$ for $5.0 \leqslant Pe \leqslant 15.0$

Peclet number	Error	$\theta = \pi/4$	$\theta = \pi/3$	$\theta = \pi/2$
5.0	$j = 4$	0.026959	0.072930	0.237637
	$j = 6$	0.001386	0.006103	0.035693
	$j = 8$	0.000088	0.000744	0.010866
10.0	$j = 4$	0.041270	0.112223	0.352307
	$j = 6$	0.004419	0.019761	0.109688
	$j = 8$	0.000107	0.000526	0.003873
15.0	$j = 4$	0.048947	0.134486	0.419533
	$j = 6$	0.006809	0.031047	0.171973
	$j = 8$	0.000509	0.003549	0.023897

can be carried out using an appropriately accurate series approximation to Eq. (16).

References

[1] W.M. Adams, Nuclear reactor apparatus for earth penetration, US Patent No. 3,115,194, 1963.
[2] A. Ansari, S. Morris, The effects of a strongly temperature-dependent viscosity on Stokes's drag law: experiments and theory, J. Fluid Mech. 159 (1985) 459–476.
[3] G.M. Benson, Thermal underground penetrator, US Patent No. 3,396,806, 1968.
[4] S.H. Emerman, D.L. Turcotte, Stokes's problem with melting, Int. J. Heat Mass Transfer 26 (11) (1983) 1625–1630.
[5] D.J. Cedio–Fengya, J.G. Stevens, Extending the integral method by symbolic computation, Proc. of the Joint Conf. on Information Sciences 1 (1998) 121–125.
[6] T.R. Goodman, Application of integral methods to transient nonlinear heat transfer, in: T.F. Irvine Jr., J.P. Hartnett (Eds.), Advances in Heat Transfer, Vol. 1, Academic Press, New York, 1964, pp. 51–122.
[7] E. Kamke, Differentialgleichungen (1958) 24–28.
[8] D. Langford, The heat balance integral method, Int. J. Heat Mass Transfer 16 (1973) 2424–2428.
[10] M.K. Moallemi, R. Viskanta, Melting around a migrating heat source, J. Heat Transfer 107 (1985) 451–458.
[11] M.K. Moallemi, R. Viskanta, Experiments on fluid flow induced by melting around a migrating heat source, J. Fluid Mech. 157 (1985) 35–51.
[12] M.K. Moallemi, R. Viskanta, Analysis of close-contact melting heat transfer, Int. J. Heat Mass Transfer 29 (6) (1986) 855–867.
[13] M.K. Moallemi, R. Viskanta, Analysis of melting around a moving heat source, Int. J. Heat Mass Transfer 29 (8) (1986) 1271–1282.
[14] S. Morris, The effects of a strongly temperature-dependent viscosity on slow flow past a hot sphere, J. Fluid Mech. 124 (1982) 1–26.
[15] N.C. Rasmussen, J. Yellin, D.J. Kleitman, R.B. Stewart, Nuclear power: can we live with it?, Tech. Rev. 81 (1979) 32–46.
[16] H. Schlichting, K. Gersten, Boundary Layer Theory, eighth ed., Springer-Verlag, New York, 1999.